Interface between Link and System Level Simulations for Downlink MC-CDMA Cellular Systems

Abdel-Majid Mourad, Arnaud Guéguen, and Ramesh Pyndiah*

Mitsubishi Electric ITE, Telecommunications Research Laboratory, Rennes, France
*** Ecole Nationale Supérieure des Télécommunications de Bretagne, Brest, France**
{mourad, gueguen}@tcl.ite.mee.com, pyndiah@enst-bretagne.fr

Abstract – **The aim of the interface between link and system level simulations is to provide accurate link level modeling to the system level simulations. The link level modeling consists mainly in defining an appropriate link quality metric (LQM) that is easy to evaluate at the system level and that can be directly mapped to the average bit (BER) and frame (FER) error rates. This paper presents an accurate and low complexity average value link to system level interface for MC-CDMA systems in the downlink. The term "average value" refers to when the observation time scale is large compared to the channel coherence time. This corresponds to the practical cases where the packet size is large and/or the Doppler spread is large. Such preliminary study is a first step in order to assess the impact of the MC-CDMA physical layer algorithms on the system capacity, which is crucial for system design.**

Keywords - **MC-CDMA, Link to system interface, Interference modeling.**

1. Introduction

Multi-Carrier Code Division Multiple Access (MC-CDMA) schemes are considered as potential candidates for the air interface of 4G wireless communication systems in the downlink [10][11]. In the literature [1]-[3], performance evaluation of the MC-CDMA physical layer algorithms has mainly been carried out at the link level, i.e. the single radio link performance are evaluated. The link performance are usually evaluated via Monte-Carlo simulations that estimate the achieved bit (BER) and frame (FER) error rates for a given scenario that specifies the physical layer parameters and multi-path channel model. The BER and FER metrics are oriented in the user perspective since they express the degree of link satisfaction. However, since the system should be designed from the provider perspective [8], it is crucial to evaluate the impact of the physical layer algorithms at the system level, i.e. when all radio links in the system are considered.

The typical system level performance metric is the system capacity, which is generally defined as the maximum amount of links that can be serviced simultaneously with satisfied quality of service (QoS) requirements [9]. In the aim of quantifying the impact of the physical layer algorithms on the system capacity, the QoS requirements can simply and reasonably be expressed in terms of a target FER to achieve. Thus, in order to evaluate the system capacity, one needs to measure the FER for each link at the system level. The problem that arises here is that performing Monte-Carlo simulations for each link at the system level in order to measure the FER results in very complex simulations. At the system level, one needs therefore to define an accurate and easy-to-evaluate link quality metric (LQM) that can be directly mapped to the BER and FER. This is the main concern of the interface between link and system level simulations [7][8].

This study investigates the average value link to system level interface for MC-CDMA schemes in the downlink of a multi-cellular environment. The term "average value" refers to when the observation time scale is large compared to the channel coherence time. This corresponds to the practical cases where the packet size is large and/or the Doppler spread is large. In this study, the local mean signal to interference plus noise ratio (SINR) taken at the output of the single user detector (SUD) is first shown to be an appropriate LQM that can be directly mapped to the average BER and FER. The term "local mean SINR" refers to when averaging over the fast fading. Thanks to interference modeling, an accurate and low complexity interface simulator is then proposed in order to provide the mappings between the local mean SINR at the output of the SUD and average FER.

The rest of this paper is organized as follows. Section 2 describes the MC-CDMA physical layer in the downlink. Section 3 presents a theoretical analysis in the aim of defining an appropriate LQM at the system level. Next, in Section 4, an accurate and low complexity interface simulator is proposed in order to provide the mappings between the defined LQM and the average BER and FER. Numerical results are then provided in Section 5, and finally, conclusions and perspectives are drawn in Section 6.

2. MC-CDMA System Description

The MC-CDMA system is considered in a multi-cellular environment made up of Q cells, each having its own base station (BS). The downlink is considered, where each BS_q transmits to K_q mobile stations (MS). Figure 1 depicts a block diagram of the MC-CDMA physical layer in the downlink.

2.1. MC-CDMA Downlink Transmitter

At the transmitter, the information bits of each active link are first encoded and bit interleaved, and then mapped to data symbols. After allocating the transmission powers for the active links, the data symbols of each link are spread with its assigned Walsh-Hadamard spreading code [1]. Next, chip-wise

summation is performed over the chips of all links, and the resulting chips are then mapped to the time and frequency bins according to the chip mapping strategy. In the literature [1][2], two chip mappings are generally envisaged. The first mapping transmits the CDMA chips of one data symbol on independently faded sub-carriers, whereas the second mapping transmits the chips on highly correlated faded sub-carriers. It is clear that the first mapping achieves higher diversity than the second mapping to the detriment of higher multiple access interference (MAI). After chip mapping, the chips are chip-wise multiplied by a random subset of the BS pseudo-noise (PN) scrambling code in order to reduce the inter-cell interference. The scrambled chips are then sent to the OFDM modulator, which performs the IFFT operation and then inserts the guard interval. Next, the signal is RF modulated and then sent through the multi-path channels of the active links.

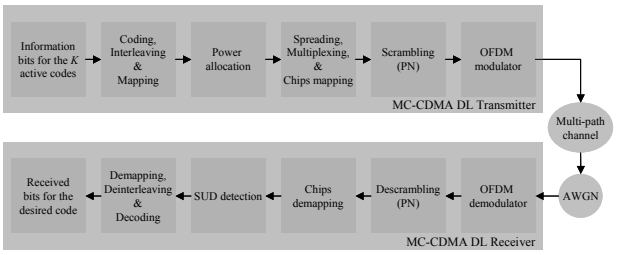

Figure 1: Block diagram of the downlink MC-CDMA physical layer.

2.2. MC-CDMA Downlink Receiver

In addition to thermal noise, the signal received by MS_k is the summation of the multi-user signals coming from all the Q BS. The maximum delay of all received signals is assumed smaller than the guard interval duration so that there is no inter-symbol interference. At the receiver side, the signal is first OFDM-demodulated by removing the guard interval and applying the FFT operation. Then, descrambling is performed, and the resulting chips are then demapped according to the chip mapping strategy employed by the transmitter. Next, single user detection (SUD) is performed in order to detect the desired signal of MS_k. SUD detection consists in a chip-per-chip equalization followed by a despreading [1]. The typical equalization strategies that have been considered in the literature are [1]-[3]: Equal Gain Combining (EGC), Maximal Ratio Combining (MRC), and Minimum Mean Square Error Combining (MMSEC). After SUD detection, the decision variables stream is first symbol demapped, and then deinterleaved and channel decoded to recover the transmitted binary information.

3. Theoretical analysis

At the output of the SUD detector, the decision variable is the summation of four terms: useful signal, intra-cell interference, inter-cell interference, and thermal noise. We consider the k-th link L_{0k} connected to BS_0. The contribution of the signal transmitted by BS_q to its j-th link L_{qj} in the decision variable d_{0k} can be written as:

$$I_{0k}^{(qj)} = \sqrt{G_{0k}^{(q)} P_{qj}} \left(\sum_{n=0}^{SF-1} W_{0q}[n] C_{0k}^{(qj)}[n] \rho_{0k}^{(q)}[n] \right) d_{qj} \qquad (1)$$

$$W_{0q} = W_q \circ W_0,\ C_{0k}^{(qj)} = C_{qj} \circ \overline{C_{0k}},\ \rho_{0k}^{(q)} = h_{0k}^{(q)} \circ z_{0k}$$

where P_{qj} and d_{qj} are respectively the transmission power and data symbol for L_{qj}. $G_{0k}^{(q)}$ and $\{h_{0k}^{(q)}\}$ are respectively the path gain and channel coefficients for the link between BS_q and the mobile station of the link L_{0k}. W_q is the scrambling code assigned to BS_q and C_{qj} is the spreading code assigned by BS_q to L_{qj}. Finally, $\{z_{0k}\}$ are the equalization coefficients derived from the channel coefficients $\{h_{0k}^{(0)}\}$, SF is the spreading factor, n is a chip index, and the symbol ° represents a chip-wise product.

The useful signal is equal to $I_{0k}^{(0k)}$, while the intra-cell interference is the summation of the terms $I_{0k}^{(0j)}$ for $j \neq k$ and $j \leq K_0$, and the inter-cell interference is the summation of all terms $I_{0k}^{(qj)}$ for $q = 1\ldots Q\text{-}1$ and $j \leq K_q$. On the other hand, the noise signal is equal to:

$$N_{0k} = \sum_{n=0}^{SF-1} T[n] W_0[n] \overline{C_{0k}}[n] z_{0k}[n] \qquad (2)$$

where $\{T\}$ are independent complex-valued Gaussian distributed random variables with zero mean and variance σ_T^2. The following assumptions are made in the sequel:

a) The spreading factor SF is sufficiently large ($SF \geq 32$) and the period P of the scrambling codes is very large when compared to SF.

b) The subset of W_q involved in the descrambling operation starts at index r_q that is uniformly distributed in [0,P-1].

c) The transmitted symbols $\{d_{qj}\}$ are normalized, i.e. with a statistical power equal to 1.

d) The channel coefficients before and after equalization are wide sense stationary.

e) Statistical averages are taken over the characteristics of data symbols, channel coefficients (fast fading process), and scrambling codes, whereas powers and path gains are fixed.

3.1. Interference Modeling

Considering the intra-cell interference, it is obvious that for a large cell load K_0, the Central Limit Theorem (CLT) applies to the intra-cell multiple access signal at the transmitter side. Thus, the complex-valued Gaussian random variable $X[n]$ models well the n-th chip of the intra-cell multiple access signal:

$$\sum_{j \neq k}^{K_0} \sqrt{P_{0j}}\, d_{0j} C_{0j}[n] \longleftrightarrow X[n] \qquad (3)$$

Instead of assuming independent random variables $\{X\}$, we propose an orthogonal Gaussian noise (OGN) model that preserves the orthogonality between the intra-cell multiple access and desired signals at the transmitter. The OGN model is characterized by the following [10]:

$$X[n] = B[n] - C_{0k}[n]\sum_{\ell=0}^{SF-1} B[\ell]\overline{C_{0k}}[\ell] \quad (4)$$

where $\{B\}$ are independent zero mean complex-valued Gaussian distributed random variables of variance σ_B^2.

Considering the inter-cell interference, it is clear that if we assume a large number of interfering cells, the CLT applies to the inter-cell interference at the input of the receiver. The n-th chip of the inter-cell interference can therefore be modeled by a complex-valued Gaussian random variable $Y[n]$:

$$\sum_{q=1}^{Q-1}\sqrt{G_{0k}^{(q)}}h_{0k}^{(q)}[n]W_{0q}[n]\left(\sum_{j=1}^{K_q}\sqrt{P_{qj}}d_{qj}C_{qj}[n]\right) \longleftrightarrow Y[n] \quad (5)$$

By assuming that the random variables $\{Y\}$ are independent, the inter-cell interference can therefore be modeled by an additive white Gaussian noise (AWGN) at the input of the receiver.

3.2. Analysis of the Bit Error Probability

By replacing the intra-cell multiple access and inter-cell interference by their OGN and AWGN models respectively, the decision variable can be written as:

$$\hat{d}_{0k} = I_{0k}^{(0k)} + \sqrt{G_{0k}^{(0)}}\left(\sum_{n=0}^{SF-1} X[n]\overline{C_{0k}}[n]\rho_{0k}^{(0)}[n]\right) + \sum_{n=0}^{SF-1}\left(Y[n]+T[n]\right)W_0[n]\overline{C_{0k}}[n]z_{0k}[n] \quad (6)$$

In the subsections below, for the sake of clarity, we omit the index $0k$ referring to the link L_{0k}.

A) Case without Channel Coding

Without channel coding, the decision variables are used by the threshold detector to recover the transmitted data. Without loss of generality, by assuming QPSK symbol mapping, the bit error probability can be expressed as:

$$P_b = \Pr\left(\mathrm{Re}(\hat{d}) > 0 \,\middle|\, \mathrm{Re}(d) = \frac{-1}{\sqrt{2}}\right) = \Pr(Z > 0) \quad (7)$$

Thus, P_b can be directly derived from the statistical distribution of the random variable Z.

In the context of low channel coefficients correlation, the CLT applies to both the intra-cell and inter-cell interference plus noise in (6), which justifies their Gaussian distributions. Moreover, by applying the Law of Large Numbers (LLN) to the useful signal, one can easily show that P_b can be simply expressed as:

$$P_b = Q\left(\sqrt{SINR}\right) \quad (8)$$

where SINR stands for the local mean signal to total interference plus noise ratio *at the output of the SUD detector*. Thus, in this context, the SINR is an appropriate link quality metric since it is directly mapped to P_b via the constant function Q. Here, note that the total interference plus noise received power $\alpha\sigma_B^2+\beta\sigma_{Y+T}^2$, where α and β are parameters that are derived from (6), fully characterizes the impact of the total interference plus noise on the bit error probability.

In the context of significant correlation, neither the CLT nor the LLN applies, and therefore, the distribution of Z becomes specific to the given scenario that defines the channel coefficients correlation, the equalization technique, and the couple of variances $(\sigma_B^2,\sigma_{Y+T}^2)$. Here, the couple of variances $(\sigma_B^2,\sigma_{Y+T}^2)$ or equivalently the couple $(\alpha\sigma_B^2+\beta\sigma_{Y+T}^2,\ \sigma_B^2/\sigma_{Y+T}^2)$ fully characterizes the impact of the total interference plus noise on the bit error probability. This leads us to state that for a given scenario that defines the channel coefficients correlation and equalization technique, P_b can be directly determined from the knowledge of the couple (SINR,Ω), where Ω stands for the ratio $\sigma_B^2/\sigma_{Y+T}^2$. This means that in this context different mappings between the SINR and bit error probability may exist for different values of Ω, and the larger the difference between these mappings is, the less appropriate the SINR metric becomes.

B) Case with Channel Coding

With soft-input channel decoding, the estimated soft inputs are used to recover the transmitted information bits. The soft inputs of the bits b_1 and b_2 mapped to the QPSK data symbol d are given by their log-likelihood ratios (LLR), which are found as:

$$\lambda_1 = \frac{2\sqrt{2}U\ \mathrm{Re}(\hat{d})}{\sigma_B^2 R + \sigma_{Y+T}^2 S}, \quad \lambda_2 = \frac{2\sqrt{2}U\ \mathrm{Im}(\hat{d})}{\sigma_B^2 R + \sigma_{Y+T}^2 S} \quad (9)$$

where the coefficients U, R, and S are coefficients that are derived from the equalization channel coefficients $\{z\}$ and equalized coefficients $\{\rho\}$.

Since there is no explicit form for the bit error probability, we make the analysis on the basis of the pair-wise error probability $P_2(\delta)$ between two neighboring channel codewords represented by two trellis paths separated by a Hamming distance δ. This analysis especially holds for convolutional codes but it can be extended to other types of linear codes with some adaptations. The pair-wise error probability averaged over the fast fading can be expressed as:

$$P_2(\delta) = E_H\left\{\Pr\left(\sum_{m=1}^{\delta}\lambda_m > 0 \,\middle|\, b_m = 0, H\right)\right\} = E_H\left\{\Pr(Z_c > 0 \,|\, H)\right\} \quad (10)$$

where H denotes a fast fading channel realization, i.e. a given set of the channel coefficients affecting the bits in the codeword, and the index m runs over the set of δ differing bits. Assuming perfect interleaving and sufficient independent samples in the set of channel coefficients affecting the bits in the codeword, the variables $\{\lambda_m\}$ can therefore be assumed independent, and consequently, the CLT applies to the variable Z_c for large δ, and thus justifies its Gaussian distribution. The pair-wise error probability $P_2(\delta|H)$ conditioned on the fast fading channel realization H can therefore be written as:

$$P_2\left(\delta\middle|H\right)=Q\left(\sqrt{\sum_{m=1}^{\delta}SINR_{m|H}}\right) \quad (11)$$

In the context of low channel coefficients correlation, the LLN applies to the coefficients U, R, and S, and therefore, the $SINR_{m|H}$ is nearly constant and equal to the local mean SINR:

$$SINR_{m|H}\approx\frac{E_H\left\{U_{m|H}^2\right\}}{\sigma_B^2E_H\left\{R_{m|H}\right\}+\sigma_{Y+T}^2E_H\left\{S_{m|H}\right\}}=SINR \quad (12)$$

The pair-wise error probability $P_2(\delta)$ averaged over the fast fading is therefore given by:

$$P_2\left(\delta\right)=Q\left(\sqrt{\delta\,SINR}\right) \quad (13)$$

Thus, in this context of channel coding with low channel coefficients correlation, the local mean SINR at the output of the SUD detector is justified analytically as an appropriate LQM. However, in the context of significant channel coefficients correlation, the LLN does not apply to the variables U, R, and S, and consequently, the local mean SINR cannot be justified analytically as an appropriate LQM that can be directly mapped to the pair-wise error probability. In this context, similarly to the case without channel coding, we assume that the knowledge of the couple (SINR,Ω) is sufficient to determine the bit error probability.

In Section 5, numerical results show that as expected the parameter Ω has negligible influence on the SINR-FER mapping in the context of low channel coefficients correlation. However, in the context of significant correlation, a more important variation is observed, but this variation is not significant so that one can still consider only one SINR-FER mapping without significant loss of accuracy in any relevant scenario for assessing system performance. This leads us to conclude that the local mean SINR at the output of the SUD detector is an appropriate LQM for any level of channel coefficients correlation.

3.3. Evaluating the SINR at the System Level

Using the property of orthogonality between the spreading codes and the assumption of wide sense stationary equalized channel coefficients, the variance of the mutual intra-cell interference $I_{0k}^{(0j)}$ in (1) can be exactly expressed as $P_{0j}G_{0k}^{(0)}\alpha_{0k}^{(0j)}$, where [5]:

$$\alpha_{0k}^{(0j)}=\Gamma_{0k}[0]\mathrm{A}_{0k}^{(0j)}[0]+2\,\mathrm{Re}\left(\sum_{n=1}^{SF-1}\Gamma_{0k}[n]\mathrm{A}_{0k}^{(0j)}[n]\right) \quad (14)$$

Γ_{0k} and $\mathrm{A}_{0k}^{(0j)}$ are respectively the statistical correlation of the equalized channel coefficients $\{\rho_{0k}^{(0)}\}$ and the aperiodic correlation of the chip-wise product code $C_{0k}^{(0j)}$ [5].

Assuming maximum length PN sequences for scrambling codes, one can easily find the following equation:

$$E\left\{W_{0q}[n]W_{0q}[m]\right\}=\left(1+\frac{1}{P}\right)\delta_{nm}-\frac{1}{P} \quad (15)$$

where δ_{nm} denotes the Kronecker symbol which is equal to 1 for $n = m$, and 0 otherwise. Equation (15) makes use of the two following properties of PN m-sequences [4]:

1) The summation of all chips in the whole period of an m-sequence is equal to –1.
2) The chip-wise product of two different m-sequences is an m-sequence different from both initial sequences.

From (1) and (15), the mutual inter-cell interference power is found equal to $P_{qj}G_{0k}^{(q)}\alpha_{0k}^{(qj)}$, where:

$$\alpha_{0k}^{(qj)}\approx\frac{\beta_{0k}}{SF},\quad \beta_{0k}=E\left|z_{0k}[n]\right|^2 \quad (16)$$

Equation (16) makes use of the independence between $\{z_{0k}\}$ and $\{h_{0k}^{(q)}\}$ for $q \neq 0$, and the fact that the channel coefficients $\{h_{0k}^{(q)}\}$ are normalized, i.e. with statistical power equal to 1. Finally, from (2), the noise signal power can be found equal to $\beta_{0k}\sigma_T^2$. The local mean SINR at the output of the SUD detector for the link L_{0k} can therefore be expressed as follows:

$$SINR_{0k}=\frac{P_{0k}G_{0k}^{(0)}\alpha_{0k}^{(0k)}}{G_{0k}^{(0)}\sum_{j\neq k}^{K_0}P_{0j}\alpha_{0k}^{(0j)}+\beta_{0k}\left(\frac{1}{SF}\sum_{q=1}^{Q-1}G_{0k}^{(q)}P_q+\sigma_T^2\right)} \quad (17)$$

Thanks to analytical derivation of $\alpha_{0k}^{(qj)}$ and β_{0k} (cf. (14) and (16)), the local mean SINR can be easily and accurately evaluated at the system level.

4. Link To System Interface Simulator

The link to system level interface simulator aims at providing the mappings between the local mean SINR and the average BER and FER. Two approaches are compared for the link to system interface simulator: Multi-link and single-link approaches. Figure 2 illustrates a block diagram of the interface simulator for both approaches. At the input of the interface simulator, one should specify the physical layer configuration, multi-path channel model, target SINR λ, cell load K, and AWGN variance σ_{Y+T}^2. At the output, the simulator provides the received SINR and the average BER and FER by running the Monte-Carlo link level simulation over several frames experiencing independent fades.

In the multi-link approach, the intra-cell multiple access signal is fully generated at the transmitter for a cell load of K active links. The inter-cell interference plus noise is modeled with an AWGN at the input of the receiver. The transmission powers for the K active links are allocated such that the SINR for each link (code) is equal to the input target SINR λ:

$$SINR_k=\frac{P_k\alpha_k^{(k)}}{\sum_{j\neq k}^{K}P_j\alpha_k^{(j)}+\beta_k\sigma_{Y+T}^2}=\lambda,\ \forall k=1\ldots K \quad (18)$$

where $\{\alpha_k^{(j)}\}$ and β_k denote respectively the orthogonality and noise factors given in (14) and (16), and P_k is the power transmitted to the k-th code. The

output BER and FER are obtained by averaging over the BER and FER of the K active links.

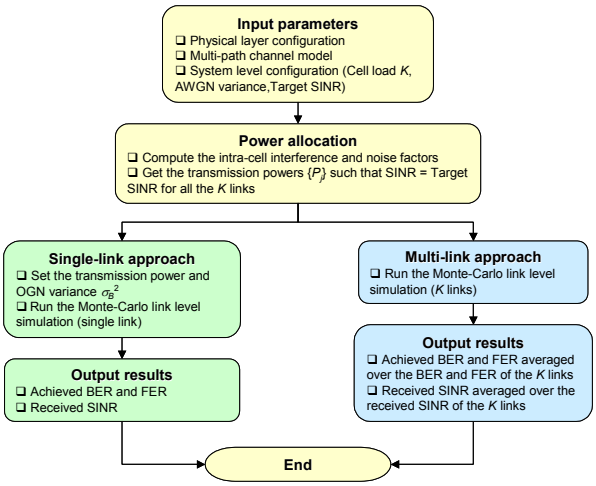

Figure 2: Block diagram of the link to system interface simulator.

In the single-link approach, the OGN model is used to generate the intra-cell multiple access signal at the transmitter (cf. Section 3.1). The inter-cell interference plus noise is modeled with an AWGN at the input of the receiver. The OGN variance σ_B^2 is found from (3) and (4) such that the intra-cell multiple access power is equal to that as when the BS has K active links, each having its SINR equal to the target SINR:

$$\sigma_B^2 = \frac{1}{SF-1}\sum_{j\neq k}^{K} P_j \qquad (19)$$

In (19), without loss of generality, the code $k = 1$ is considered. The powers $\{P_j\}$ are the solutions of (17). Note that the powers $\{P_j\}$ in (19) are intermediate parameters that are used only to determine σ_B^2. On the other hand, the useful transmission power within the single-link interface simulator is called P_u, and is found such that the received SINR is equal to λ:

$$SINR = \frac{P_u \alpha_1^{(1)}}{\alpha_1 \sigma_B^2 + \beta_1 \sigma_{Y+T}^2} = \lambda \qquad (20)$$

where $\alpha_1 = \Gamma_1[0] - \alpha_1^{(1)}$ denotes the OGN intra-cell interference factor, and Γ_1 is the statistical correlation of the equalized channel coefficients (cf. (14)).

It is important to note that (18), (19) and (20) ensure that the multi-link and single-link approaches have the same values of the target SINR, intra-cell multiple access power, and AWGN variance. At last, we should point out that the single-link approach has the advantage of being much less complex and time consuming than the multi-link approach, which on the other hand benefits from an exact generation of the intra-cell multiple access signal.

5. Numerical Results

The key parameters of the MC-CDMA physical layer in the downlink are summarized in [10]. The propagation environment is modeled with the urban ETSI BRAN E channel, which has a coherence bandwidth of approximately 4 MHz and a maximum Doppler frequency of 233 Hz [10]. Two frequency domain chip mappings are considered, namely adjacent (AFM) and interleaved (IFM) frequency mappings. IFM represents the context of low channel coefficients correlation, whereas AFM represents the context of significant correlation. In the following, results are presented in terms of the SINR-BER mappings. It is important to note that the same conclusions are also valid for the SINR-FER mappings.

Channel coding	Convolutional (R = ½, g_1 = 753, g_2 = 561)
Symbol mapping	QPSK-Gray mapping
Spreading codes	Hadamard (SF = 32)
Chip mapping	¤ Scenario 1: Interleaved frequency mapping ¤ Scenario 2: Adjacent frequency mapping
FFT size	1024
Sampling frequency	57.6 MHz
Occupied bandwidth	41.45 MHz
Channel model	ETSI BRAN E [10]
Receiver type	SUD - MMSEC

Table 1: Simulation parameters.

Figure 3 and Figure 4 depict the SINR-BER mappings obtained from both single-link and multi-link approaches and for two different values of K (or equivalently Ω): K = 16 (half cell load) and K = 32 (full cell load). Figure 3 considers the context of low channel coefficients correlation (IFM), whereas Figure 4 considers the context of significant channel coefficients correlation (AFM).

As shown in Figure 3, the SINR-BER mapping is almost invariant with respect to K (or equivalently Ω) in the IFM context. This result can be expected from the analysis done in Section 3.2, where it is proved analytically that in the context of low channel coefficients correlation, the local mean SINR is directly mapped to the bit error probability. In Figure 4, the SINR-BER mappings obtained for K = 16 and K = 32 can be clearly distinguished, which means that in this context of significant correlation, the influence of K on the SINR-BER mapping is not negligible. However, one can observe that the difference between the SINR-BER mappings obtained for K = 16 and K = 32 is less than 0.5 dB. Thus, for medium to large cell loads, one can still consider only one SINR-BER mapping without significant loss of accuracy. For instance, by considering the mapping obtained for K = 24, the error is found to be negligible in the IFM context and less than 0.25 dB in the AFM context for less than 10^{-3} BER. This means that for medium to large cell loads, one can still consider only one SINR-BER mapping without significant loss of accuracy. Thus, by confining our analysis to the range between medium and full cell loads, which is the critical context to assess system performance, one can state that the influence of the cell

load K (or equivalently Ω) on the SINR-BER mapping can be neglected for any level of channel coefficients correlation. This leads us to conclude that the local mean SINR is an appropriate link quality metric at the system level in any relevant scenario for assessing system performance.

On the other hand, in Figure 3 and Figure 4, one can observe that the SINR-BER mappings obtained from both single-link and multi-link approaches are very close in all cases. This means that the OGN model is valid for any level of channel coefficients correlation. The SINR-BER mappings can therefore be provided from the interface simulator by using the single-link approach, which is much less complex and time consuming than the multi-link approach.

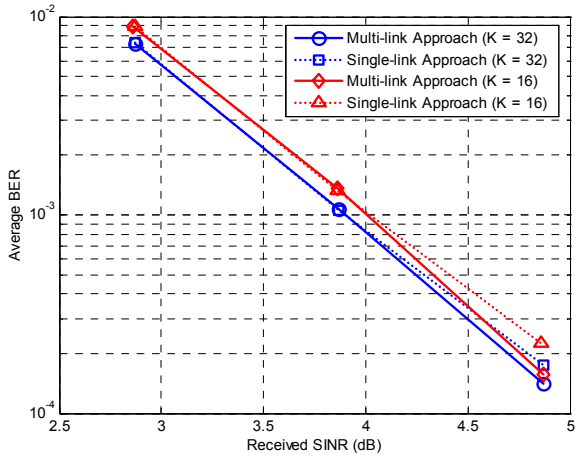

Figure 3: Average BER versus local mean SINR for both multi-link and single-link approaches in the context of low channel coefficients correlation.

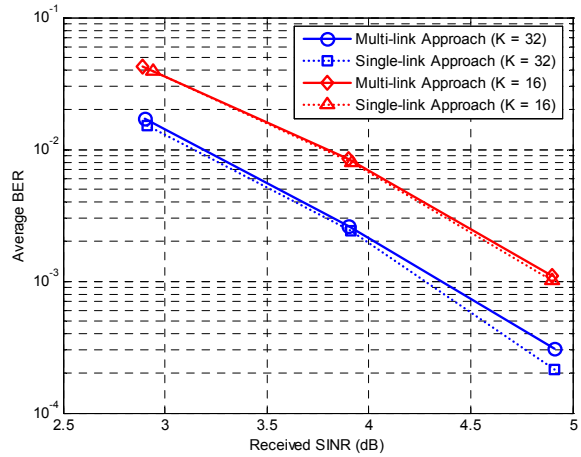

Figure 4: Average BER versus local mean SINR for both multi-link and single-link approaches in the context of significant channel coefficients correlation.

6. Conclusions and Perspectives

This paper has presented an accurate average value interface between link and system level simulations for MC-CDMA systems in the downlink. The local mean SINR taken at the output of the SUD detector has been shown to be an appropriate link quality metric at the system level. Thanks to analytical derivation of the interference factors, the local mean SINR can be easily and accurately evaluated at the system level. Moreover, thanks to interference modeling, an accurate and low complexity single link interface simulator has been proposed to provide the SINR-BER and SINR-FER mappings. These mappings should be provided for each scenario that defines the physical layer configuration and multi-path channel model. At the system level, these mappings will be used to convert the FER requirements for link satisfaction into requirements on the SINR, while the interference factors will be used to evaluate the SINR. The system capacity can then be estimated by solving the problem of finding the maximum amount of links that can be serviced simultaneously with satisfied local mean SINR requirements. Future work will be devoted to quantify the impact of the MC-CDMA physical layer algorithms on the downlink system capacity, which is crucial for system design.

7. Acknowledgment

The work presented in this paper was supported by the European IST project 4More (4G MC-CDMA multiple antenna system On chip for Radio Enhancements) [11].

8. References

[1] S. Hara and R. Prasad. "*Design and Performance of Multi-carrier CDMA System in Frequency-Selective Rayleigh Fading Channels*". IEEE Transactions on Vehicular Technology, Vol. 48, No. 5, September 1999.

[2] A. Persson et al. "*Utilizing the channel correlation for MAI reduction in downlink multi-carrier CDMA systems*". Proceedings of Radio Vetenskap och Kommunikation 2002, June 2002.

[3] K. Fazel and S. Kaiser. "*Multi-Carrier and Spread Spectrum Systems*". John Wiley & Sons Ltd, 2003.

[4] P. Fan and M. Darnell. "*Sequence Design for communications applications*". Research Studies Press Ltd., 1996.

[5] A.M. Mourad et al. "*MAI Analysis for Forward Link Mono-Dimensionally Spread OFDM Systems*". IEEE Vehicular Technology Conference Spring 2004, Milan, May 2004.

[6] S. Hälmäläinen et al. "*A Novel Interface Between Link and System Level Simulations*". Proceedings of ACTS Summit 1997, Aalborg, October 1997.

[7] H. Holma. "*A Study of UMTS Terrestrial Radio Access Performance*". Ph.D. dissertation, Helsinki University of Technology, October 2003.

[8] J. Zander et al. "*Radio Resource Management For Wireless Networks*". Artech House Publishers, 2001.

[9] UMTS 30.03 version 3.2.0. "*Selection Procedures for the Choice of Radio Transmission Technologies of the UMTS*". ETSI TR 101 112 V3.2.0, 1998.

[10] IST-MATRICE, http://ist-matrice.org.

[11] IST-4MORE, http://ist-4more.org.